

Halogen-substituted salicylhydroximate copper(II) metallacrowns: from synthesis and structures to novel applications

Marina A. Katkova, Galina S. Zabrodina, Roman V. Rumyantcev, Grigory Yu. Zhigulin, Maria S. Muravyeva, Margarita P. Shurygina, Sergey A. Chesnokov and Sergey Yu. Ketkov

1. Experimental

General Procedures

All chemicals were reagent-grade and were used as received from Sigma Aldrich without any additional purification. The 5-chloro-, 5-bromo- and 5-iodo-substituted salicylhydroxamic acids were synthesized from 5-halogenosalicylic acid as described [F. Cao *et al.*, *Inorg. Chem.* 2013, **52**, 10747]. The C, H, N elemental analyses were performed by the Microanalytical laboratory of IOMC RAS on Euro EA 3000 Elemental Analyser. IR spectra were obtained on a Perkin Elmer 577 spectrometer and recorded from 4000 to 450 cm^{-1} as a Nujol mulls on KBr pellets. Electronic absorption spectra were recorded with the Perkin Elmer Lambda 25 UV/Vis spectrophotometer at room temperature, at 200–1100 nm. NMR spectra were acquired using the Bruker Avance III 400 MHz NMR spectrometer. All NMR spectra were acquired at room temperature. The photopolymerization process was carried out under irradiation of low-energy light sources LEDs@385,405 nm exposure (25 mW cm^{-2}), $T = 298$ K, in air. FTIR spectra were measured from 4000 to 500 cm^{-1} at a resolution of 4 cm^{-1} by the FT-801 spectrometer with a TR attachment with diamond crystal of NPR ‘Simex’, Novosibirsk, Russia. The double-bond conversion was calculated using the area under the C=C peak at 1646 cm^{-1} . Because the methyl-group of the methacrylic fragment content does not change during photopolymerization, the CH_3 peak at 1450 cm^{-1} was used as an internal standard in the FTIR analysis. Each curve of polymerization was an average result of three experiments differing in maximum superficial polymerization rate and limiting conversion by no more than 10%.

A general synthesis for the **1–4** complexes based on the 5- R substituted salicylhydroxamic acid (R= -H, -Cl, -Br, -I) is described below for complex **1**. The **2–4** complexes were prepared similarly by using 5- halogen substituted instead of unsubstituted salicylhydroxamic acid.

Synthesis of $(\text{Bu}_4\text{N})_2[\text{Cu}|\text{2-MC}_{\text{CuN}(\text{shi})}-\text{4}]\text{J}$ (1)

Copper(II) acetate dihydrate (0.25 g, 1.25 mmol) was dissolved in MeOH-DMF solvent mixture. Salicylhydroxamic acid (shiH₃; 0.153 g, 1 mmol) was added, and this was allowed to stir for 0.5 h during which time the dark green solution aging. Then, 40% water solution Bu₄NOH (0.33 ml, 0.5 mmol) was added dropwise, and the resulting mixture was stirred for 3 h before green-brown solid precipitated. After standing overnight, the solid was collected by centrifugation (6000 RPM) and recrystallized from DMF. Slow evaporation of the solvent yielded 0.14 g (40%) of dark-green cubes crystals. Anal. Calcd for C₆₀H₈₈Cu₅N₆O₁₂: C, 51.36; H, 6.32; N, 5.99. Found: C, 51.41; H, 6.29; N, 5.93. ¹H NMR (DMSO, 400 MHz, 298 K, δ ppm): 20.96 (br. s, 4H, C(2)H), 7.44 (br. s, 4H, C(6)H), 5.77 (br. s, 4H, C(1)H), 4.59 (br. s, 4H, C(3)H), 3.17 (m, 16H, NCH₂), 1.57 (m, 16H, CH₂), 1.32 (m, 16H, CH₂), 0.94 (t, $J=7.2$, 24H, CH₃). λ_{max} (MeOH)/nm 316, 616.

Synthesis of $(Bu_4N)_2[Cu[12-MC_{CuN(Cl-shi)}-4]]$ (2)

The complex was prepared similarly to **1** by using 5-chlorosalicylhydroxamic acid (0.19 g, 1 mmol). Yield: 0.16 g (41%). Anal. Calcd for $C_{60}H_{88}Cl_4Cu_5N_6O_{14}$: C, 45.70; H, 5.63; N, 5.33. Found: C, 45.72; H, 5.59; N, 5.28. 1H NMR (DMSO, 400 MHz, 298 K, δ ppm): 19.7 (br. s, 4H, C(2)H), 7.49 (br. s, 4H, C(6)H), 4.95 (br. s, 4H, C(3)H), 3.22 (m, 16H, NCH₂), 1.63 (m, 16H, CH₂), 1.37 (m, 16H, CH₂), 0.97 (t, J =7.2, 24H, CH₃). λ_{max} (MeOH)/nm 328, 619.

Synthesis of $(Bu_4N)_2[Cu[12-MC_{CuN(Br-shi)}-4]]$ (3)

The complex was prepared similarly to **1** by using 5-bromosalicylhydroxamic acid (0.23 g, 1 mmol). Yield: 0.17 g (39%). Anal. Calcd for $C_{60}H_{88}Br_4Cu_5N_6O_{14}$: C, 41.07; H, 5.06; N, 4.79. Found: C, 41.09; H, 5.01; N, 4.71. 1H NMR (DMSO, 400 MHz, 298 K, δ ppm): 19.81 (br. s, 4H, C(2)H), 7.58 (br. s, 4H, C(6)H), 4.89 (br. s, 4H, C(3)H), 3.22 (m, 16H, NCH₂), 1.61 (q, 16H, CH₂), 1.37 (m, 16H, CH₂), 0.97 (t, J =7.2, 24H, CH₃). λ_{max} (MeOH)/nm 328, 620.

Synthesis of $(Bu_4N)_2[Cu[12-MC_{CuN(Ishi)}-4]]$ (4)

The complex was prepared similarly to **1** by using 5-iodosalicylhydroxamic acid (0.28 g, 1 mmol). Yield: 0.16 g (26 %). Anal. Calcd for $C_{60}H_{88}Cu_5I_4N_6O_{14}$: C, 41.07; H, 5.06; N, 4.79. Found: C, 41.09; H, 5.01; N, 4.71. λ_{max} (MeOH)/nm 328, 621.

Complex formation was studied by comparison of the electronic absorption spectra of the complexes with those of the free ligands. By comparison with the measured absorption maxima of the free main ligand 5-chlorosalicylhydroxamic acid at 314 nm, the bands at 338 nm of **MC** can be assigned to characteristic for a ligand-to-metal charge-transfer (LMCT) in copper(II) chlorosalicylhydroximate metallacrown and the maximum at 621 nm which represents a copper centred d-d transition.

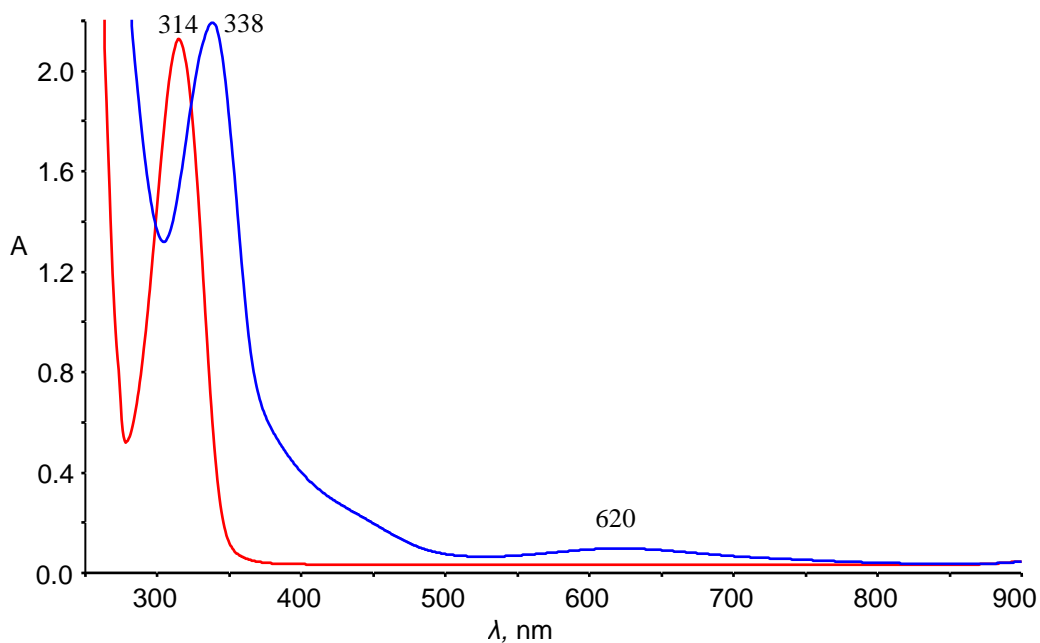


Figure S1. UV-vis spectra of the *Cl-shiH₃* ligand (c = 1 mM) (red line), and $(Bu_4N)_2[Cu[12-MC_{Cu(II)N(Cl-shi)}-4]]$ (c = 0.125 mM) in DMF (blue line).

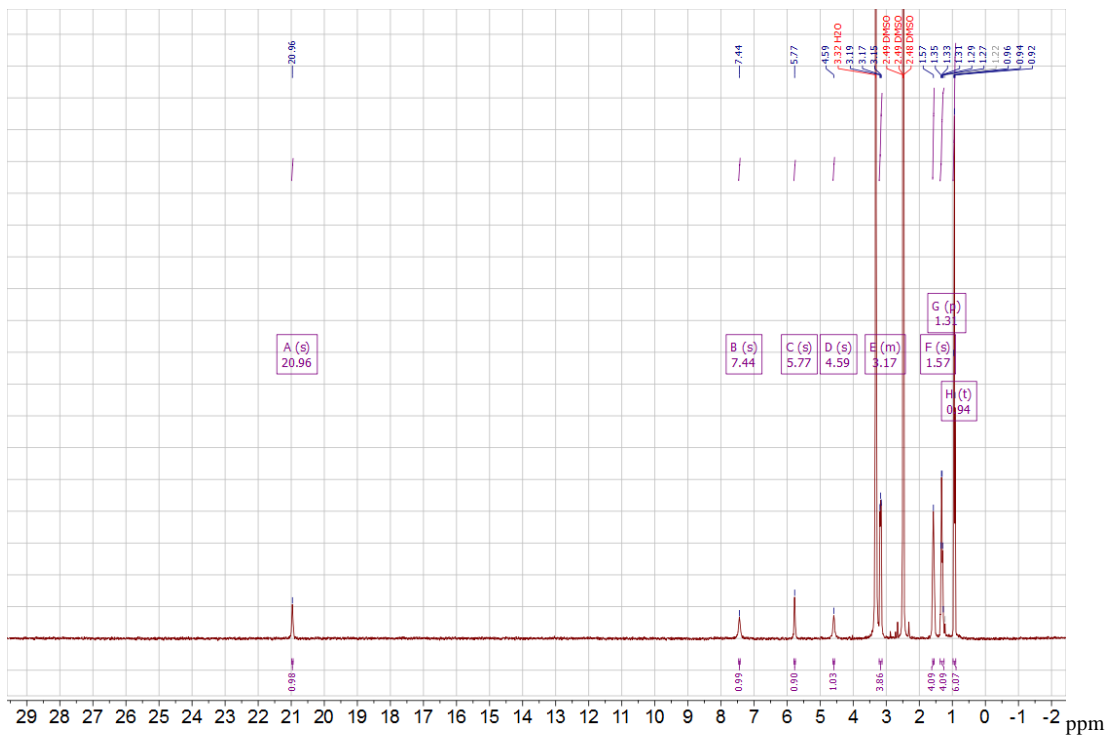


Figure S2. ^1H NMR spectrum of $(\text{Bu}_4\text{N})_2[\text{Cu}[12\text{-MC}_{\text{CuN}(\text{shi})}\text{-4}]]$ (**1**) in $\text{DMSO-}d_6$

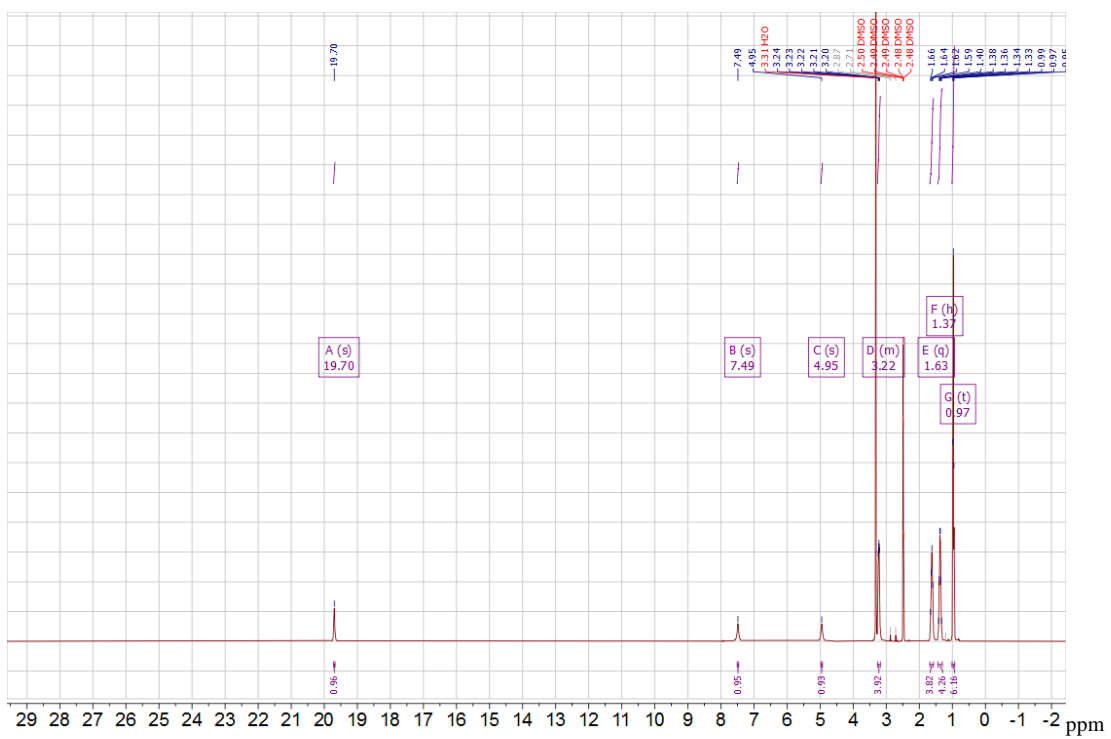


Figure S3. ^1H NMR spectrum of $(\text{Bu}_4\text{N})_2[\text{Cu}[12\text{-MC}_{\text{CuN}(\text{Clshi})}\text{-4}]]$ (**2**) in $\text{DMSO-}d_6$

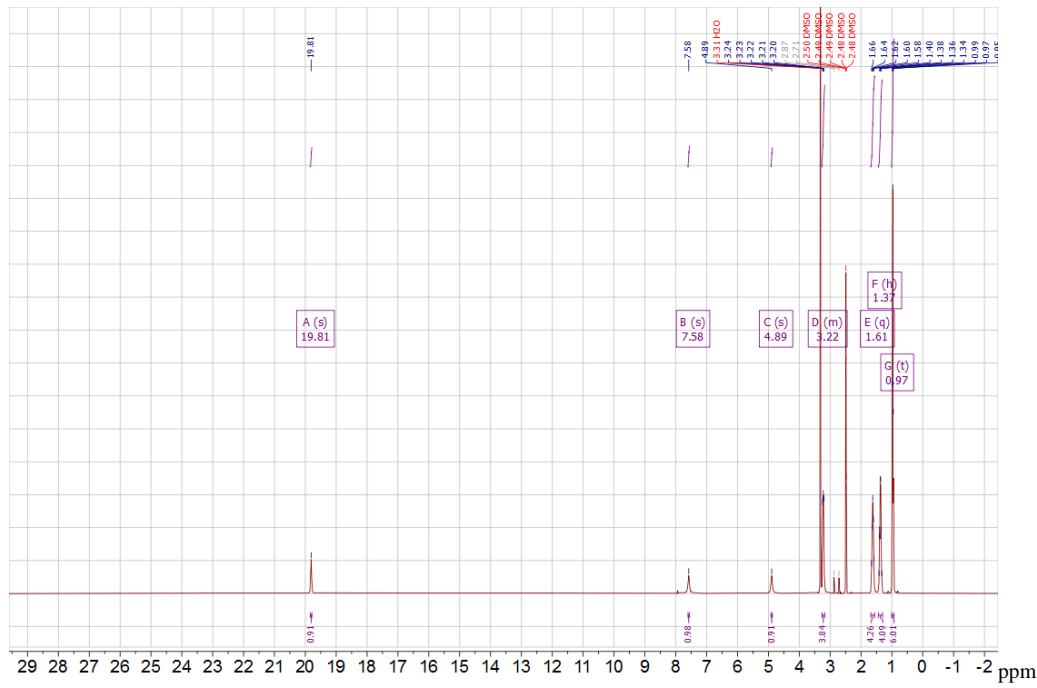


Figure S4. ^1H NMR spectrum of $(\text{Bu}_4\text{N})_2[\text{Cu}[12\text{-MC}_{\text{CuN}(\text{Brshi})}\text{-4}]]$ (**3**) in $\text{DMSO-}d_6$

Table S1. Details of crystallographic, collection and refinement data for complexes **1**, **2** and **3**

Complex	1	2	3
Empirical formula	$\text{C}_{60}\text{H}_{88}\text{Cu}_5\text{N}_6\text{O}_{12}$	$\text{C}_{60}\text{H}_{88}\text{Cl}_4\text{Cu}_5\text{N}_6\text{O}_{14}$	$\text{C}_{60}\text{H}_{88}\text{Br}_4\text{Cu}_5\text{N}_6\text{O}_{14}$
Formula weight	1403.06	1576.86	1754.70
Temperature [K]	100(2)	100(2)	100(2)
Crystal system	Monoclinic	Monoclinic	Monoclinic
Space group	P2/n	P2 ₁ /n	P2 ₁ /n
Unit cell dimensions			
a[Å]	18.6359(9)	18.6623(7)	18.8048(7)
b[Å]	8.1055(4)	18.3520(7)	18.5677(7)
c[Å]	19.8079(10)	18.8978(7)	18.8166(7)
β [°]	91.844(2)	90.0626(14)	90.9989(13)
Volume [Å ³]	2990.5(3)	6472.3(4)	6569.0(4)
Z	2	4	4
Calculated density [Mg/m ³]	1.558	1.618	1.774
Absorption coefficient [mm ⁻¹]	1.816	1.850	4.093
F(000)	1462	3260	3548
Crystal size [mm ³]	0.70×0.08×0.04	0.36×0.33×0.24	0.40×0.29×0.20
θ [°]	2.057 – 30.584	2.155 – 28.699	1.894 – 30.034
Reflections collected / unique	45566 / 9190	65947 / 16716	146346 / 19195
R(int)	0.0435	0.0562	0.0389
Final R indices	$R_1=0.0354$,	$R_1=0.0508$,	$R_1=0.0314$,
[$I>2\sigma(I)$]	wR ₂ =0.0835	wR ₂ =0.1222	wR ₂ =0.0668
R indices (all data)	$R_1=0.0490$,	$R_1=0.0872$,	$R_1=0.0459$,
	wR ₂ =0.0887	wR ₂ =0.1395	wR ₂ =0.0721
S	1.057	1.027	1.047
Largest diff. peak and hole [e/Å ³]	0.730/-0.432	1.863/-0.780	1.304/-0.953

Table S2. Selected angles ($^{\circ}$) in complexes **1**, **2** and **3**.

Angles [$^{\circ}$]	1	2	3
C-N-C(NBu ₄)	105.2(2) – 112.0(2)	106.0(2) – 111.7(2)	106.0(2) – 112.2(2)
O(oxime)-Cu(1)-O(oxime)	89.1(4) – 90.9(4); 180.0	89.0(2) – 91.8(2); 177.4(2), 179.2(2)	89.0(2) – 91.6(2); 177.6(2), 179.4(2)
O(oxime)-Cu-O(carbonyl)	80.3(3) – 80.9(4)	80.5(2) – 80.9(2)	80.7(2) – 81.0(2)
O(phenolate)-Cu-N(imine)	92.0(2) – 93.8(5)	92.2(2) – 93.9(2)	92.7(2) – 94.2(2)
O(oxime)-Cu-N(imine)	87.8(6) – 89.0(2)	89.2(2) – 90.4(2)	89.1(2) – 90.2(2)
O(phenolate)-Cu-O(carbonyl)	97.3(1) – 99.7(3)	97.0(2) – 98.6(2)	96.5(2) – 98.2(2)

* – Symmetry transformations used to generate equivalent atoms in crystal **1**: $-x+1, -y+1, -z+1$, $-x+1/2, y, -z+1/2$ and $-x+1/2, y, -z+3/2$.

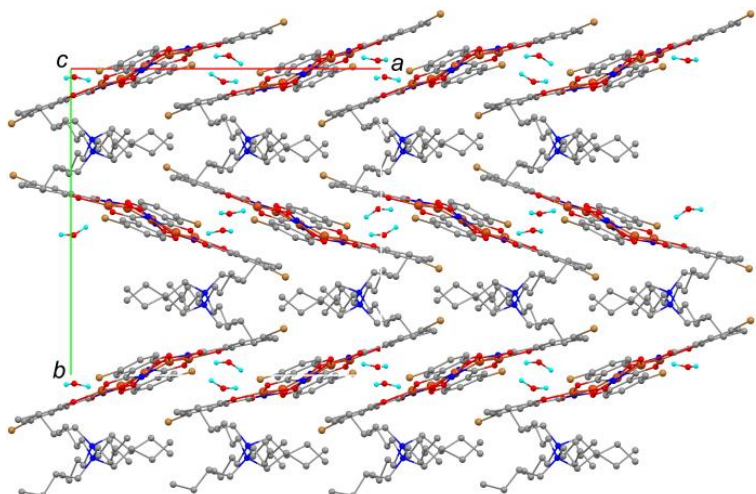


Figure S5. Fragments of crystal packing along the crystallographic *c* axis of complex **3**. The hydrogen atoms are omitted for clarity.

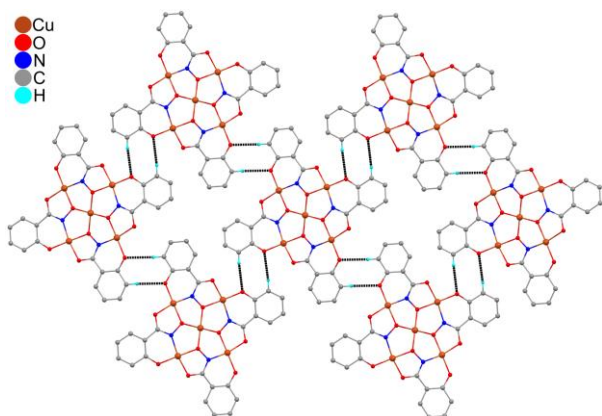


Figure S6. Fragments of anionic 2D network of complex **1**. The tetrabutylammonium cations and hydrogen atoms which are not involved in intermolecular interactions are omitted for clarity.

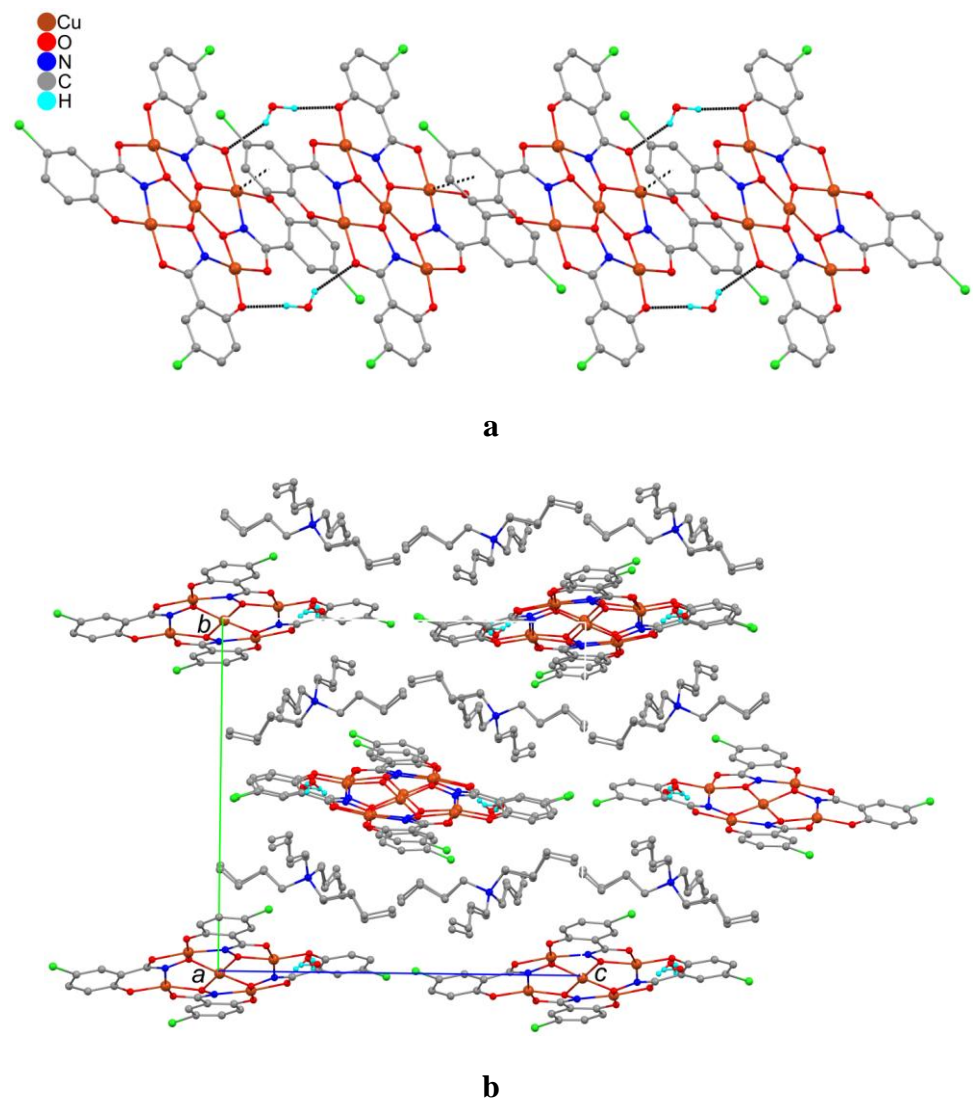
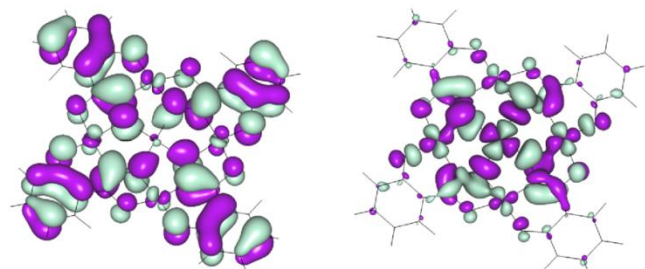
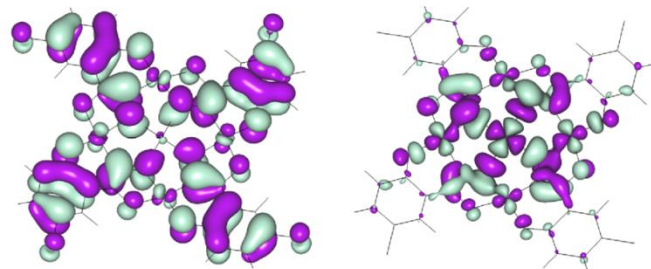


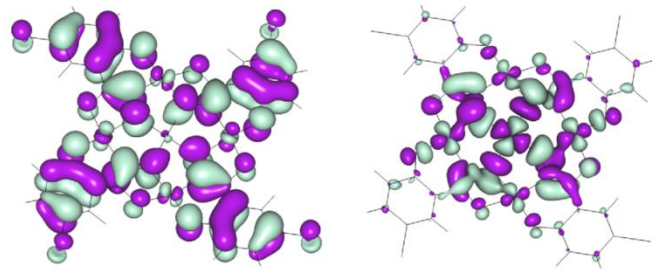
Figure S7. Fragments of anionic 1D chain (**a**) and crystal packing along the crystallographic *a* (**b**) of complex **2**. The tetrabutylammonium cations (**a**) and hydrogen atoms which are not involved in intermolecular interactions (**a** and **b**) are omitted for clarity.



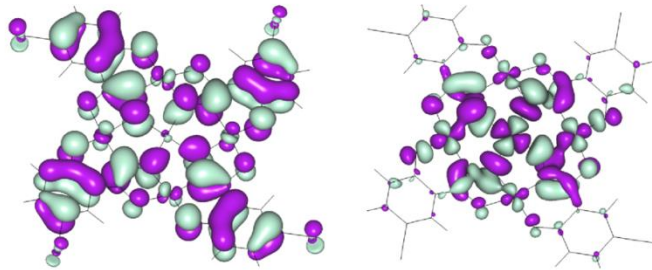
1 (H), β -HOMO, -0.89 1 (H), β -LUMO, 1.04



2 (Cl), β -HOMO, -1.34 2 (Cl), β -LUMO, 0.57



3 (Br), β -HOMO, -1.41 3 (Br), β -LUMO, 0.51



4 (I), β -HOMO, -1.49 4 (I), β -LUMO, 0.43

Figure S8. Detailed view of the MO isosurfaces (at 0.018) for the dianionic metallamacrocycles. The corresponding energies are given in eV.

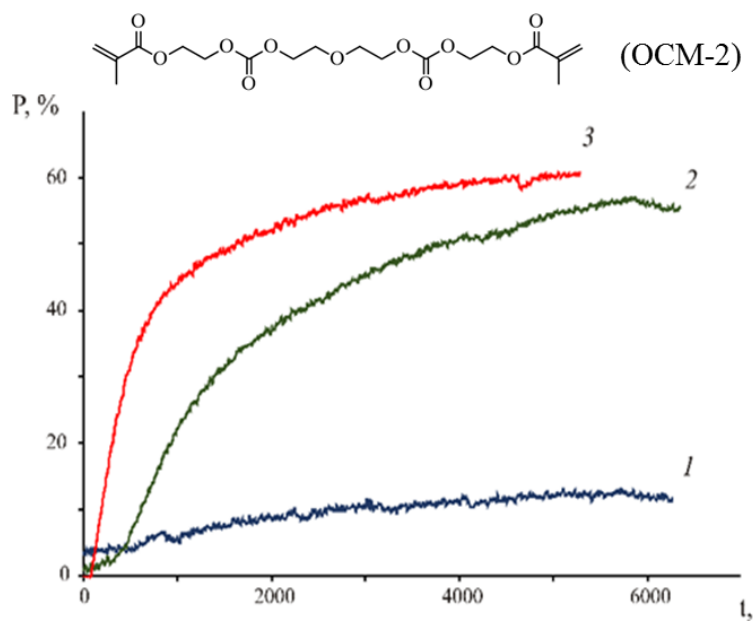


Figure S9. Kinetic curves of OCM-2 photopolymerization initiated by **3** in the presence of TEA. TEA concentration, vol.-%: 1) 0; 2) 1 and 3) 10. $[3] = 1.3 \times 10^{-4}$ M. Irradiation by LEDs 385, 405 nm (25 mW cm^{-2}), $T = 298$ K, air.